Available online at www.sciencedirect.com

ScienceDirect

Procedia CIRP 68 (2018) 22 – 27

www.elsevier.com/locate/procedia

19th CIRP Conference on Electro Physical and Chemical Machining, 23-27 April 2018, Bilbao, Spain

ED-machinable ceramics with oxide matrix: Influence of particle size and volume fraction of the electrical conductive phase on the mechanical and electrical properties and the EDM characteristics

Andrea Gommeringer[a]*, Ulrich Schmitt-Radloff[a], Philipp Ninz[a], Frank Kern[a], Fritz Klocke[b], Sebastian Schneider[b], Maximilian Holsten[b], Andreas Klink[b]

[a]*Institute for Manufacturing Technologies of Ceramic Components and Composites (IFKB), University of Stuttgart, Allmandring 7b, D-70569 Stuttgart, Germany*

[b]*Laboratory for Machine Tools and Production Engineering (WZL), RWTH Aachen University, Steinbachstraße 19, 52074 Aachen, Germany*

* Corresponding author. Tel.: +49-711-685 68234; fax: +49-711-685 58234. *E-mail address:* andrea.gommeringer@ifkb.uni-stuttgart.de

Abstract

Structural and functional properties of ceramics can be beneficial in a variety of applications. The main drawback of ceramics is their complex and costly manufacturing cycle, in particular the final machining step. For customized parts, electrically conductive ceramics represent a cost efficient alternative to conventional ceramics since electrical discharge machining (EDM) can be applied. Ceramic composites consisting of a high content of oxide matrix and a second phase that provides electrical conductivity show promising properties in wear resistance, strength, and toughness. In this study, composites with yttria stabilized zirconia as matrix material and an electrically conductive tungsten carbide dispersion (TZP-WC) were investigated. The content of the conductive phase varied from 20 to 28 vol.-% and three different particle sizes were used. Ceramic blanks were manufactured by hot pressing and then tested with respect to mechanical and electrical properties. Wire as well as sinking EDM machining characteristics were analyzed. The necessary adaptions of the EDM processing parameters to the requirements of this specific material system were investigated. The variation of the conductive phase in the observed range caused only slight variations in mechanical properties. However, a strong impact of composition on EDM characteristics was found as the contributions of different material removal mechanisms are altered. Smaller particle sizes and higher contents of electrically conductive phase generally led to higher electrical conductivity, thereby improving the machining rate at a similar surface quality.

Peer-review under responsibility of the scientific committee of the 19th CIRP Conference on Electro Physical and Chemical Machining

Keywords: electrical discharge machining; electrically conductive ceramics; mechanical properties; tetragonal zirconia; tungsten carbide

1. Introduction

Partially stabilized zirconia is well known for its excellent mechanical properties and therefore used in a variety of applications [1–3]. In particular, the uncommonly high fracture resistance and strength of tetragonal zirconia polycrystals (TZP), which are mainly caused by transformation toughening [3], make this oxide ceramic interesting for engineering applications. Although the benefits are large, in many cases other materials are chosen because of its high costs in the manufacturing cycle. Conventional hard machining of complex ceramic components suffers from geometrical restrictions. In such cases, electrical discharge machining (EDM) of ceramics is a promising approach to reduce the manufacturing cost. Composites with a strong and tough TZP matrix and a percolating electrically conductive carbide dispersion (such as tungsten carbide, WC), are known ED-machinable materials [4,5]. A sufficiently high electrical conductivity is widely accepted to be the prerequisite for electrical discharge machining [6]. Bonny et al. has already mentioned the ED-machinability and has shown some first results for the material system zirconia / tungsten carbide [7].

In the present study, the main aim is to investigate the effects of material composition (volume fraction and grain size of

Peer-review under responsibility of the scientific committee of the 19th CIRP Conference on Electro Physical and Chemical Machining
doi:10.1016/j.procir.2017.12.016

conductive phase) on material removal mechanisms during EDM to develop a set of suitable process parameters. Further investigations tend to identify the lower limit of carbide content for economical ED-machinability. In the ZTA-TiC system Landfried has already investigated on the changes in ED-machinability when using carbide a phase of different grain sizes at volume contents close to the percolation threshold [8]. Lauwers has demonstrated different removal mechanisms in different material systems, such as evaporation, melting and re-solidification and spalling [9]. The surface quality strongly depends on the removal mechanisms and probably has an effect on the mechanical properties of the finished part [9,10]. In this study, the main objective is to fabricate ED-machinable ceramics with a high content of oxide matrix by using fine grained and homogeneously dispersed carbide dispersions, to benefit from the excellent mechanical properties of the TZP matrix.

2. Experimental procedure

2.1. Sample manufacturing and mechanical characterization

Hot pressed samples with different amount and particle size of the electrically conductive phase were investigated. The starting powders for the powder preparation of the composite material were partially stabilized zirconia (TZ-3Y-SE, Tosoh, Japan) and tungsten carbide of three different particle sizes (WC DN4.0, d_{50} = 0.3 µm; WC DN2.5, d_{50} = 0.6 µm; WC DS60, d_{50} = 0.7 µm, H.C. Starck, Germany). The specified particle sizes were analyzed by laser granulometry (Mastersizer 3000, Malvern Instruments GmbH, Germany). Nine different batches of 600 g were blended by mixing and milling for 2 h in 500 ml isopropanol using 1300 g Y-TZP milling balls (2 mm diameter). The solvent was evaporated at 50 °C for 24 h and the residue was screened through a 90 µm mesh. Cylindrical discs of 2.3 mm thickness and 40 mm diameter were hot pressed at 1450 °C and 60 MPa axial pressure for 2 h. In addition samples with a thickness of 5 mm for sinking experiments and 10 mm for wire EDM experiments were pressed. The surfaces were prepared by lapping and polishing with 15, 6, 3 and 1 µm diamond suspension. The mechanical characterization included measurements of density, Vickers hardness (HV 10, Bareiss, Germany), Young's modulus (acoustic method, IMCE Belgium), 4-point bending test (Zwick, Germany outer span 20 mm, inner span 10 mm, crosshead speed 0.5 mm/min), and fracture resistance by indentation strength in bending (ISB) method (the residual strength of a HV10 indented sample was measured in the same 4-point setup at 2.5 mm/min crosshead speed). The phase composition of zirconia was measured by X-ray diffraction (X'Pert MPD, PANalytical GmbH, Germany, Bragg-Brentano theta-2theta, copper source, $K\alpha_1$) and calculated by integration of the -111 (monoclinic) and 101 (tetragonal) reflections. SEM images were taken of polished and thermally etched samples (1200 °C, 6 min, forming gas with 5 % hydrogen) at 3 kV acceleration voltage (Zeiss Gemini, Germany, in lens) to analyze the grain size of the zirconia matrix.

2.2. Wire and sinking EDM experiments

Wire EDM experiments were conducted on a GFMS Cut 2000 oiltech. A coated brass wire Bedra topas plus H was used as the wire electrode and oelheld IonoFil was used as the dielectric. To examine the cutting rate test cuts with a length of s = 8 mm were done and only the main cut was analyzed. To assure constant flushing conditions in each test cut, a triangular shape was machined prior to the test cut, see Figure 1.

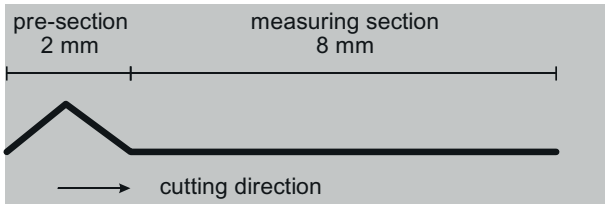

Figure 1: Cutting geometry of wire EDM experiments.

The fundamental machining parameters, listed in Table 1, are *I* as parameter for the discharge current and *P* as discharge power parameter, which affects the discharge frequency. *I* influences the discharge current depending on the adjusted cutting technology and workpiece height. Other parameters, such as *ISH*, S_{soll}, and *Reg*, have impact on the machining condition control: The *ISH* value offers to regulate the pulse duration, if excessive short circuit discharges occur. S_{Soll} is the set point for the feedback control of the feed rate. *Reg* decides the way of controlling the feed (*Reg* = 0…15 feedback; *Reg* = 20…30 open loop). The real current and voltage were measured with Tektronix probes in combination with a Tektronix DPO7109C oscilloscope. Microscopy was conducted with the laser scanning microscope Keyence VK-X250.

Table 1: Machining parameters of wire EDM experiments.

Parameter	I	P	S_{soll}	ISH	Reg
Value	7	30	30	-1	0

Sinking EDM experiments were carried out on a GFMS FORM 2000 VHP machine tool using electrolytic copper electrodes with a cross section of A_{el} = 5 * 5 mm^2 and a plunging depth of t_N = 1 mm. Oelheld IonoPlus IME-MH was the oil based dielectric used. In case of very low removal rates, experiments were stopped at the processing time t_H = 30 min.

The determination of removal and wear rates were conducted gravimetrically by weight measurements of both tool and workpiece before and after machining.

Table 2 presents the standard values for the sinking EDM technology as proposed by the manufacturer: Discharge duration t_e, discharge current i_e, pulse interval time t_0, open circuit voltage $\hat{u}_i$, erosion time between retraction flushing movements t_{eros} and the dimensionless servo parameter *servo* (possible range: $0 < servo < 1$) which affects the desired ignition delay time as an input of the servo control. The standard tool polarity was negative.

Table 2: Machining parameters of sinking EDM experiments.

Parameter	t_e	i_e	t_0	$\hat{u}_i$	t_{eros}	servo
Value	5.6 µs	6.2 A	24 µs	250 V	0.2 s	0.25

3. Results

3.1. Microstructure and phase transformation of zirconia

Figure 2 shows SEM images of the composite material containing 20, 24 and 28 vol.-% WC (left to right) manufactured with tungsten carbide of different grain size (coarse to fine: left to right). WC grains were strongly attacked by the thermal etching. Figure 2a shows a very large WC grain embedded in TZP. As the second phase suppresses the grain growth of the matrix, increasing grain size and decreasing volume fraction of the dispersion go along with a coarsening of the matrix (see Figure 3).

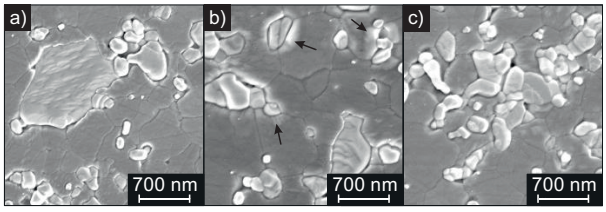

Figure 2: SEM images of composite material containing
a) coarse TZP-20WC, b) medium TZP-24WC and c) fine TZP-28WC.

Figure 2b shows phase transformation of the zirconia grains at TZP/WC grain boundaries. As this was not observed in polished and non-etched surfaces, which are entirely tetragonal (see Figure 3), it can be assumed that this effect is an artefact of the thermal etching. Figure 2c shows the composite material with the finest WC starting powder, which contains a great amount of agglomerated subgrains.

X-ray measurements were carried out to analyze the phase composition of polished surfaces representing the bulk material. The same measurements applied on fracture surfaces, served to calculate the transformability during failure. The volume fraction of the monoclinic zirconia phase was calculated by the equations (1) and (2) first published by Toraya [11].

$$V_m = \frac{1.311 X_m}{1 + 0.311 X_m} \quad (1)$$

$$X_m = \frac{I_{m(-111)} + I_{m(111)}}{I_{m(-111)} + I_{m(111)} + I_{t(101)}} \quad (2)$$

V_m is the volume fraction of monoclinic phase and X_m is the intensity fraction of the monoclinic phase. $I_{m/t}$ are the intensities of the reflexes itself. As the second monoclinic reflex (111) at $2\theta = 31.468°$ overlaps with a reflex of WC (001) only the first monoclinic reflex (-111) at $2\theta = 28.175°$, can be applied for calculation of monoclinic content. The intensity distribution of the monoclinic reflexes are 100% at $2\theta = 28.175°$ and 68% at $2\theta = 31.468°$ (reference pattern JCPDS 07-0343 [12]). Resulting from that, it can be assumed that $I_{m(111)} = 0.68\ I_{m(-111)}$. The results of the calculation are shown in Figure 3.

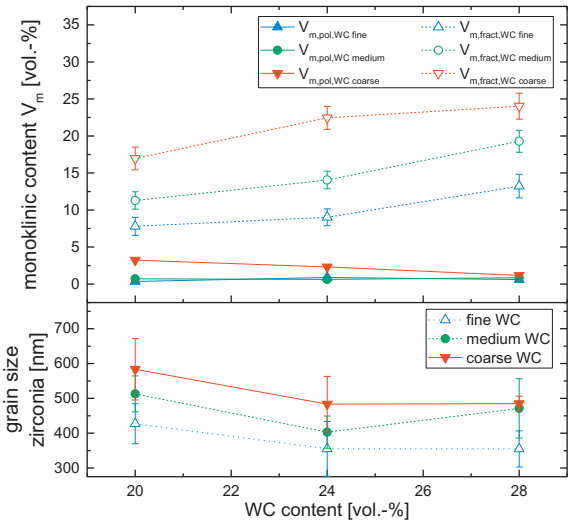

Figure 3: Bottom: Grain size of the zirconia matrix in the composite material; top: monoclinic phase content of zirconia measured at polished surfaces $V_{m,\,pol}$ and fracture faces $V_{m,\,fract}$.

As shown in Figure 3, the grain size decreases with increasing carbide content and depends on its particle size. Larger WC grains lead to larger zirconia grains and induce stronger tensile residual stress on the zirconia grains in their vicinity. Thus the grain size thus influences the tetragonal to monoclinic (t-m) transformation. This causes increasing transformability with increasing carbide content and carbide particle size. However, the impact of the t-m transformability on the fracture toughness was almost negligible since only slight changes in the fracture toughness were measured, see Table 3.

3.2. Mechanical and electrical properties

Figure 4 shows the results of the measurements of Vickers hardness, 4-point-bending strength and the electrical conductivity. Electrical conductivity increased with increasing amount of WC phase. The composites manufactured with coarse WC powder provided much less conductivity at the same level of WC volume fraction. This phenomenon is explainable by the higher percolation of the WC phase at small particle sizes. Thus, the electrical conductivity increases with decreasing grain size of the WC phase. The composite material containing 28 vol.-% WC with the finest starting powder should provide the highest electrical conductivity according to this theory. The deviation from this theoretical prediction may be explained by the high degree of agglomeration of the fine WC powder (Figure 2c).

Evidently, the hardness increased with increasing volume fraction of WC phase, caused by the much harder tungsten carbide (21.8 GPa [13]). Due to the finer dispersion at smaller WC particles, the hardness also increased with decreasing particle size.

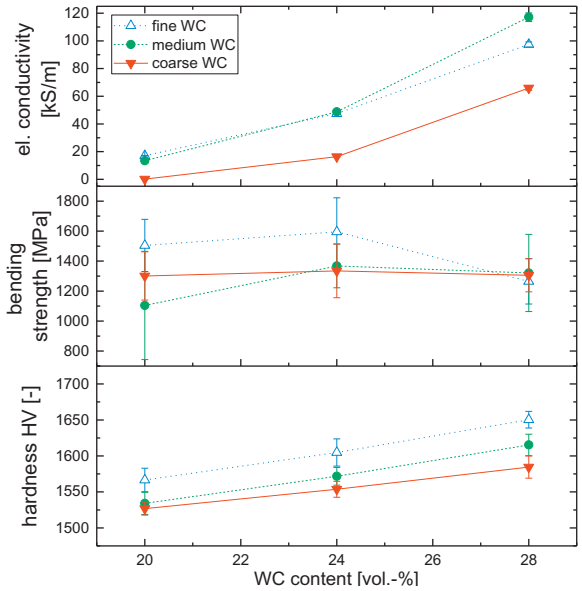

Figure 4: Top: electrical conductivity; centre: 4-point bending strength; bottom: Vickers hardness of the composite material.

The bending strength for fine and medium tungsten carbide composites first increased with increasing WC content from 20 to 24 vol.-%, then decreased at higher contents. The bending strength for coarse tungsten carbide remained at a constant level of 1300 MPa and was essentially unaffected by the carbide content. Composites manufactured from the finest tungsten carbide powder achieved the highest strength of 1600 MPa (24 vol.-% fine WC). The fracture toughness K_{Ic}, shown in Table 3, increased with increasing particle size of WC. This was probably caused by crack deflection at the larger grains and incrementally improved transformation toughness. The variation of tungsten carbide content at identical grain size does not cause significant changes of toughness.

The measurements of the density (not shown) exhibit that all samples were fully dense (> 99.5%). As a result, the hot pressing parameters can be considered sufficient to obtain dense materials. The increase of Young's modulus (see Table 3), with increasing volume fraction of WC from 270 GPa to about 290 GPa qualitatively follows the rule of mixture (*E(Y-TZP)* = 210 GPa [14], *E(WC)* = 737 GPa [13]).

Table 3: Mechanical and electrical properties.

sample	Young's modulus [GPa]	el. conductivity [S/m]	bending strength [MPa]	$K_{Ic,\ ISB}$ [MPa $m^{1/2}$]
3Y-TZP-20WC fine	269	17000	1505	5.3
3Y-TZP-20WC medium	265	13500	1104	5.5
3Y-TZP-20WC coarse	267	120	1301	5.7
3Y-TZP-24WC fine	273	45000	1595	5.4
3Y-TZP-24WC medium	279	49000	1368	5.5
3Y-TZP-24WC coarse	281	16400	1334	5.8
3Y-TZP-28WC fine	290	72300	1228	5.5
3Y-TZP-28WC medium	293	117000	1321	5.5
3Y-TZP-28WC coarse	295	66000	1306	5.8

3.3. ED-machinability

The machinability by EDM depends on the electrical conductivity of the composite. Depending on literature, the minimum electrical conductivity is about σ_e = 1…10 S/m [15]. For economically machining processes a higher conductivity is necessary. In the top of Figure 4 the different conductivities of the investigated material compositions are shown.

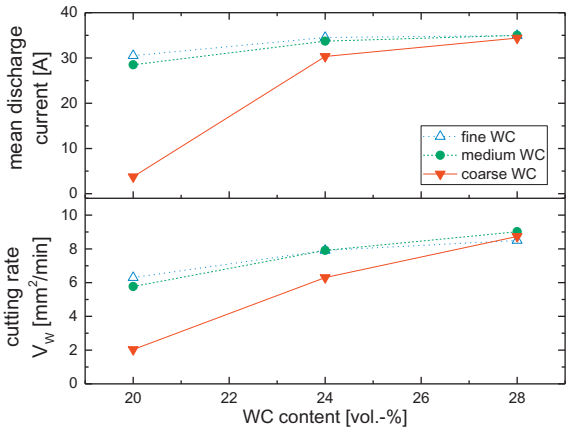

Figure 5: Results wire EDM experiments (I = 7, P = 30): Top: mean discharge current; bottom: cutting rate.

Figure 5 shows the measured cutting rates for the different composite materials. The composite material with coarse particles and a WC-content of 20 vol.-% which has the lowest electrical conductivity, was machinable with the lowest cutting rate. The relevant surface topography is shown in Figure 6 in comparison to the surface with a good machinable material. The cutting rate of the other material compositions could be classified in two levels: The fine and medium grained composites with the lowest WC-content of 20 vol.-% and the coarse grained TZP-24WC led to similar cutting rates of about V_W = 5.7…6.3 mm²/min. Compared to the deviation of the electrical conductivity (σ_e = 9.96…12.6 kS/m), changes in the cutting rates are found to be in an equal magnitude. This indicates a great influence of the electrical conductivity on the electrical discharge removal mechanism in the order of magnitude of 5-15 kS/m. The other materials had a significantly higher conductivity (σ_e > 35 kS/m) which, however, has only a moderate impact on the achievable cutting rates (V_W = 8…10 mm²/min). The discharge currents confirmed the results of cutting rate analysis (see Figure 5).

Figure 6 shows the topography of the eroded surfaces from both extreme points: a) coarse grained with lowest WC-content and b) fine grained with the highest WC-content. The coarse TZP-20WC had a considerably rougher and more inhomogeneous appearance. It manifests large burn marks caused by flashover. Additionally, the fine grained TZP-28WC, such as the other investigated materials (not shown), developed a smooth surface with a homogeneous roughness. The measured arithmetic mean roughness values *Ra* confirms this impression. Figure 7 presents that all composite material had a mean roughness of *Ra* = 0.86…1.42 µm except for coarse TZP-20WC, which reached a mean roughness of

Ra = 2.51 µm. A smaller particle size led to a decrease of the mean roughness, hence the composite material with 28 vol.-% WC and a particle size of 0.3 µm reached the lowest roughness (*Ra* = 0.86 µm).

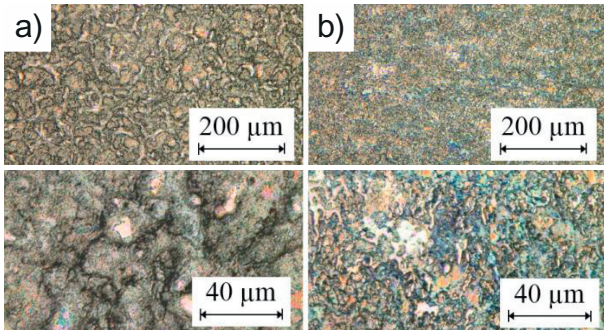

Figure 6: Wire ED-machined surface topography of a) 3Y-TZP-20WC coarse and b) 3Y-TZP-28WC fine.

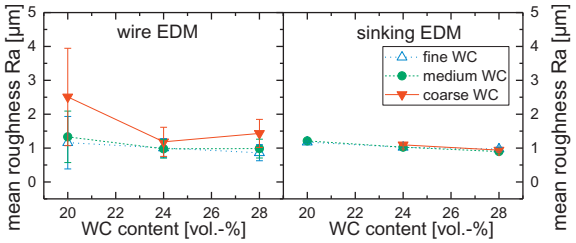

Figure 7: Surface mean roughness of wire (left) and sinking (right) EDM experiments.

In sinking EDM experiments material removal rates highly correlated with the electrical conductivity for 20 and 24 vol.-% WC-content, see Figure 8. Furthermore, the removal rate increased with a decrease of WC particle size. The composite material with coarse TZP-20WC was not machinable by sinking EDM since the material fractured during the first discharges. As a result, the observations in sinking were essentially similar to observations in wire cutting EDM.

Surface roughness measurements revealed a decrease of roughness *Ra* with an increase of the WC content, but no significant influence of WC grain size; the results are shown in Figure 7. Laser scanning microscopy was carried out on low, medium and high WC content ceramics (not shown). A smoother surface at higher WC-contents results from a decreased size of the crater borders. Furthermore, similar surface cracks occur on all samples.

Maximum removal rates achieved were in the range of $V_W < 0.35$ mm^3/min, these are comparably low rates. Thus, parameters were optimized to increase the removal rates. An increase of the erosion time between the retraction movement/ flushing cycles increased the active process time, but reduced overall flushing efficiency. This approach (increasing erosion time t_{eros} from 0.2 s to 0.3 s) did not lead in a notable increase of the removal rate.

Electrical signal analyses revealed that the technology included an additional pulse interval time of $t_0 = 470$ µs after nine discharges. Thereby additional deionization of the gap within the flushing cycle was achieved. In order to increase the discharge frequency, this additional interval time was removed. As a result the removal rate was approximately doubled to values up to $V_W = 0.76$ mm^3/min and the volumetric relative wear was reduced significantly from 4 % to 0.9 % (medium TZP-24WC). Another step towards increasing the removal rate was to change the servo regulation parameter, which sets a desired value for the ignition delay time with an antiproportional correlation. By increasing this value the removal rate was further increased up to $V_W = 1.83$ mm^3/min at a negligible increase of relative wear to 0.5 % (medium TZP-24WC).

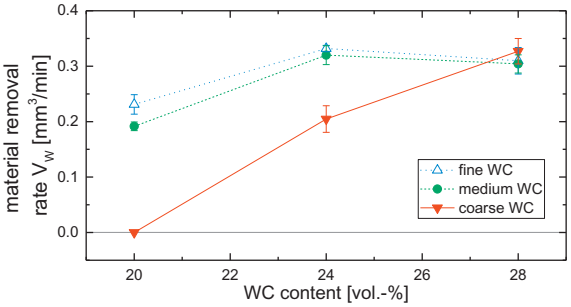

Figure 8: Material removal rates of sinking EDM experiments.

4. Conclusion

Fully dense zirconia / tungsten carbide composites were produced by hot pressing. Wire and sinking EDM experiments were performed. With respect to the mechanical properties, all samples reached a sufficient level for engineering applications. The hardness increased with increasing WC-content and decreasing particle size from 1530 for coarse TZP-20WC to 1650 for fine TZP-28WC. The bending strength reached values up to 1600 MPa (fine TZP-24WC). The toughness measured by ISB increased moderately with increasing particle size and content of the carbide phase from 5.3 MPa m$^{1/2}$ for fine TZP-20WC to 5.8 MPa m$^{1/2}$ for coarse TZP-28WC. Additional toughness was caused by enhanced crack deflection at larger WC grains. As the grains of the zirconia matrix coarsened with decreasing WC content and grain size, larger WC grains caused a higher transformation toughness increment. It was found that higher fracture resistance can be triggered e.g. by reducing the stabilizer concentration or shifting from coprecipitated to stabilizer coated TZP powders. As expected, the electrical conductivity increased with carbide phase content and decreasing carbide particle size due to the rules of percolation. The deviation from this trend for the finest WC powder at higher WC-contents was probably caused by hard agglomeration of the ultrafine powder (see Figure 2c).

Wire EDM experiments showed that all samples are ED-machinable. Results indicated that at low carbide fractions the machinability extremely depends on the WC grain size. Compared to coarse TZP-20WC, where the cutting rate was 2 mm^2/min, the cutting rates for the finer TZP-20WC samples rose to 6 mm^2/min and reached the level of samples with higher WC-content. The results of mean discharge current measurements and surface analysis confirmed this trend. The surface roughness of well machinable TZP-WC exhibited a

smooth surface with $Ra = 0.86\,\mu m$ at a cutting rate of 8.5 mm^2/min.

Compared to wire EDM, sinking EDM experiments showed similar correlations, except for the coarse TZP-20WC composite, which was not machinable at all. Using standard EDM parameters the measured material removal rate reached only moderate values in the range of 0.2 to 0.33 mm^3/min for all other samples. This comparably low rate was significantly improved by an adaption of the erosion technology. By elimination of an additional pulse interval time after nine discharges, the material removal rate reached 0.76 mm^3/min. Further improvement was obtained by increasing the servo regulation parameter, which was not set to an optimal value for the machining of TZP-WC ceramics in the standard technology. A servo regulation parameter adjusted for shorter ignition delay times increased the material removal rate to $V_W = 1.83$ mm^3/min. Further experiments will be required to analyze the influence of the technology parameters in detail.

Acknowledgements

The authors gratefully acknowledge the funding of the project by the German Founding Organization (DFG), grant numbers KE879/3-1 and KL500/142-1, and would like to thank Mrs. Felicitas Predel from Max-Planck-Institute for Solid State Research in Stuttgart for preparing excellent SEM images.

References

[1] Garvie R, Hannik RH, Pascoe RT. Ceramic steel? Nature 1975;258(5537):703-704.

[2] Chevalier J, Gremillard L, Virkar AV, Clarke DR. The Tetragonal-Monoclinic Transformation in Zirconia: Lessons Learned and Future Trends. Journal of the American Ceramic Society 2009;92(9):1901–20.

[3] Heuer AH. Transformation Toughening in ZrO_2-Containing Ceramics. Journal of the American Ceramic Society 1987;70(10):689–98.

[4] Huang S, Vanmeensel K, Biest O, Vleugels J. Sintering, thermal stability and mechanical properties of ZrO_2-WC composites obtained by pulsed electric current sintering. Frontiers of Materials Science 2011;5(1):50–6.

[5] Jiang D, van der Biest O, Vleugels J. ZrO_2–WC nanocomposites with superior properties. Journal of the European Ceramic Society 2007;27(2-3):1247–51.

[6] König W, Dauw DF, Levy G, Panten U. EDM-Future Steps towards the Machining of Ceramics. CIRP Annals - Manufacturing Technology 1988;37(2):623–31.

[7] Bonny K, Baets P de, Vleugels J, Salehi A, van der Biest O, Lauwers B et al. Influence of secondary electro-conductive phases on the electrical discharge machinability and frictional behavior of ZrO_2-based ceramic composites. Journal of Materials Processing Technology 2008;208(1-3):423–30.

[8] Landfried R, Kern F, Gadow R. Electrically conductive ZTA–TiC ceramics: Influence of TiC particle size on material properties and electrical discharge machining. International Journal of Refractory Metals and Hard Materials 2015;49:334–8.

[9] Lauwers B, Kruth JP, Liu W, Eeraerts W, Schacht B, Bleys P. Investigation of material removal mechanisms in EDM of composite ceramic materials. Journal of Materials Processing Technology 2004;149(1-3):347–52.

[10] Munz M, Risto M, Haas R, Landfried R, Kern F, Gadow R. Machinability of ZTA-TiC Ceramics by Electrical Discharge Drilling. Procedia CIRP 2013;6:77–82.

[11] Toraya H, Yoshimura M, Somiya S. Calibration Curve for Quantitative Analysis of the Monoclinic-Tetragonal ZrO_2 System by X-Ray Diffraction. Journal of the American Ceramic Society 1984;67(6):C119-C121.

[12] McMurdie HF, Morris MC, Evans EH, Paretzkin B, Wong-NG W, Hubbard CR. Methods of Producing Standard X-Ray Diffraction Powder Patterns. Powder Diffraction 1986;1(1):40–3.

[13] Kosolapova TJ (ed.). Handbook of high temperature compounds: Properties, production, applications. New York: Hemisphere Publ. Corporation; 1990.

[14] Lange FF. Transformation toughening: Part 4 Fabrication, fracture toughness and strength of Al_2O_3-ZrO_2 composites. Journal of Materials Science 1982;17:247–54.

[15] Klocke F, König W. Fertigungsverfahren 3: Abtragen, Generieren und Lasermaterialbearbeitung. 4th ed. Springer; 2007.